J. CHEM. SOC. FARADAY TRANS., 1994, 90(21), 3221–3227

Low-temperature Kinetics of Reactions between Neutral Free Radicals

Rate Constants for the Reactions of OH Radicals with N Atoms ($103 \leqslant T/K \leqslant 294$) and with O Atoms ($158 \leqslant T/K \leqslant 294$)

Ian W. M. Smith* and David W. A. Stewart
School of Chemistry, The University of Birmingham, Edgbaston, Birmingham, UK B15 2TT

Rate constants have been determined for the reaction between OH radicals and N atoms at temperatures down to 103 K and for the reaction between OH and O atoms down to 158 K. Discharge-flow methods were used to generate known steady-state concentrations of N and O atoms in a cryogenically cooled flow of gas. OH radicals were produced, in concentrations much smaller than those of the atomic radicals, by pulsed laser photolysis of a small concentration of HNO_3 introduced into this gas flow, and their first-order kinetic decays were observed using the time-resolved laser-induced fluorescence technique. The rate constants for both reactions increase monotonically down to the lowest temperatures achievable in the present experiments but do not exhibit any simple functional dependence on temperature. It is suggested that expressions of the form: $k(T) = F_{elec}(T)(T/298)^n k'(298)$ are used to fit the data on these reactions at temperatures $\leqslant 515$ K. Here $F_{elec}(T)$ is the temperature-dependent ratio of the electronic degeneracy of the lowest potential surface, leading adiabatically from reagents to products, to the product of the electronic partition functions for the reagents, n has the value -0.17 for the N + OH reaction and -0.24 for O + OH, and the values of $k'(298)$ are 2.0×10^{-10} cm^3 molecule^{-1} s^{-1} for N + OH and 3.7×10^{-10} cm^3 molecule^{-1} s^{-1} for O + OH, and correspond to rate constants for reaction on the lowest potential-energy surface at 298 K. Because the value of $F_{elec}(T)$ for both reactions is essentially constant for $T \leqslant 50$ K, it is suggested that expressions of the form $k(T) = AT^B$ are used in chemical models of interstellar clouds with $A = 2.0 \times 10^{-10}$ cm^3 molecule^{-1} s^{-1} and $B = -0.17$ for N + OH and $A = 3.7 \times 10^{-10}$ cm^3 molecule^{-1} s^{-1} and $B = -0.24$ for O + OH.

This paper reports new kinetic measurements on the reactions of OH radicals with N and with O atoms:

$$N + OH \rightarrow NO + H; \quad \Delta_r H°(298\ K) = -203.8\ kJ\ mol^{-1} \tag{1}$$

$$O + OH \rightarrow O_2 + H; \quad \Delta_r H°(298\ K) = -70.7\ kJ\ mol^{-1} \tag{2}$$

Previous direct experiments[1–3] have established the rate constants for these reactions at temperatures between 220 and 515 K. Based on measurements made between 250 and 515 K, Howard and Smith[1] suggested that the temperature dependence of the rate constants of these reactions could be expressed by the functions:

$$k_1(T) = 5.3 \times 10^{-11}(T/298)^{-0.25}\ cm^3\ molecule^{-1}\ s^{-1}$$

$$k_2(T) = 3.8_5 \times 10^{-11}(T/298)^{-0.50}\ cm^3\ molecule^{-1}\ s^{-1}$$

In evaluating these results, and those reported by Lewis and Watson[2] and Brune *et al.*,[3] for the purposes of atmospheric chemistry, Baulch and co-workers have proposed the expressions:

$$k_1(T) = 3.8 \times 10^{-11} \exp(85/T)\ cm^3\ molecule^{-1}\ s^{-1}$$

$$k_2(T) = 2.3 \times 10^{-11} \exp(110/T)\ cm^3\ molecule^{-1}\ s^{-1}$$

for the temperature ranges 220–500 K for reaction (1) and 250–500 K for reaction (2). The experiments reported in this paper extend the kinetic data base on these reactions down to 103 K in the case of reaction (1) and to 158 K for reaction (2).

The reactions between OH and nitrogen and oxygen atoms and the reverse of these two reactions, particularly that between hydrogen atoms and O_2, play an important role in a number of complex environments including combustion systems,[5] the atmospheres of the earth and other planets,[6] and interstellar clouds.[7–13] These environments span a wide range of temperature and it is therefore important to have laboratory measurements of k_1 and k_2 over a similarly wide temperature range, not least because the factors controlling the temperature dependence of the rate constants of radical–radical reactions, especially those between reagents exhibiting considerable electronic degeneracy and near-degeneracy, are complex and only partially understood.[14]

Reactions (1) and (2) are examples of the simplest kind of non-associative reaction between free radicals and therefore serve as valuable prototypes of radical–radical reactions in general. For this reason and because of their importance in a wide variety of environments, they have received considerable attention from theoreticians. There have been numerous calculations of the potential-energy surfaces that are involved in both reaction (1)[15–20] and reaction (2).[21–25] In addition, the dynamics of both reactions have been examined by a variety of theoretical methods[26] including quasiclassical trajectories,[27–30] quantum scattering calculations,[31] transition state theories,[32] statistical adiabatic channel models,[33] and adiabatic capture theories.[34–36] In our own laboratory, the dynamics of reaction (1) have been investigated experimentally[37] by determining the nascent distribution of the NO product over its energetically accessible vibrational levels. Although the distribution is close to that predicted by statistical phase-space theories,[38,39] Smith *et al.*[37] doubted if this was evidence for reaction *via* a long-lived complex, and this conclusion appears to be confirmed by very recent trajectory calculations by Guadagnin and Schatz.[27] Rather, Smith *et al.* suggested that the tight angular-momentum constraints present in this system might necessarily lead to a distribution close to the phase-space prediction.

A major motivation for the present low-temperature measurements on reactions (1) and (2) has been our wish to improve the kinetic data base for neutral–neutral reactions used by those attempting to model the chemistry leading to molecular synthesis in interstellar clouds. Until very recently, there were very few measurements of rate constants for such

reactions below 200 K and none below 80 K. Consequently, modellers have had to rely on rough estimates of the required rate constants or the results of untested theoretical calculations. Within the last two years, a start has been made towards filling this experimental void.[40,41] Rate constants have been determined for several reactions of CN,[40] OH[41] and CH[42] radicals at temperatures as low as 13 K, using a CRESU (Cinétique de Réactions en Ecoulement Supersonique Uniforme) apparatus in which an ultra-cold gas mixture is prepared by its expansion through a Laval nozzle. As in the present experiments, the reaction is then initiated by creating radicals by pulsed laser photolysis (PLP) of a suitable radical precursor and the kinetic decays of the radicals are observed by time-resolved laser-induced fluorescence (LIF). Despite the success of this method it is clear that it will be difficult to apply it to those reactions, like (1) and (2), between two unstable free radicals. It is therefore important to obtain rate data for these prototypical radical–radical reactions down to as low a temperature as possible using more conventional techniques.

The experimental method adopted for the present measurements is based on that employed by Howard and Smith.[1] The atomic radicals are produced and their steady-state concentrations established employing standard discharge-flow techniques. The actual kinetic measurements are however made in 'real time'. A small concentration of HNO_3 is introduced into the gas flow downstream from the discharge and is partially dissociated to produce OH radicals by PLP at 266 nm. Subsequent decays in the concentration of OH are then observed using time-resolved LIF. In the experiments reported here, the flowing gas mixture could be cooled, using a variety of cryogens, to temperatures as low as 103 K. Although the design of the cell differed from those used in earlier experiments in our laboratory,[43] the general principle in the present experiments was the same as before.

Experimental

Fig. 1 shows a schematic diagram of the apparatus which was employed. The apparatus incorporates the following capabilities: (i) The generation of steady-state concentrations of N or O atoms in a flowing gas mixture and their estimation by standard discharge-flow techniques. (ii) The creation of a small concentration of OH radicals ($[OH]_0 \ll [N]$ or $[O]$) by PLP of HNO_3 which was added to the gas flow downstream from the microwave discharge cavity. (iii) The observation, by time-resolved LIF, of the decay with time of relative concentrations of OH following their creation by PLP of HNO_3. (iv) The variation of the temperature at which experiments were performed from room temperature down to *ca.* 100 K using a variety of cryogens.

The central part of the apparatus was a reaction cell which was constructed from Pyrex. In contrast to the jacketed reaction vessels used in other low-temperature measurements in our laboratory,[43] it was designed in the form of a cross and was similar to the cell used by Smith *et al.*[37] in their measurements of the NO vibrational state distribution from reaction (1). The main tube, id 40 mm and *ca.* 50 cm long, carried the gas flow and was evacuated by a high-speed rotary pump (Leybold, Trivac D40B). This tube incorporated a hollow insert through which refrigerant could flow. This insert extended for about 10 cm before and after the observation zone at the centre of the cross formed by the main flow tube and the side-arms through which the laser beams entered and left the apparatus. There was a gap of *ca.* 3 cm between the two sections of the cooling insert before and after the observation zone, allowing the beams from the photolysis and probe lasers unimpeded access to the gas flow.

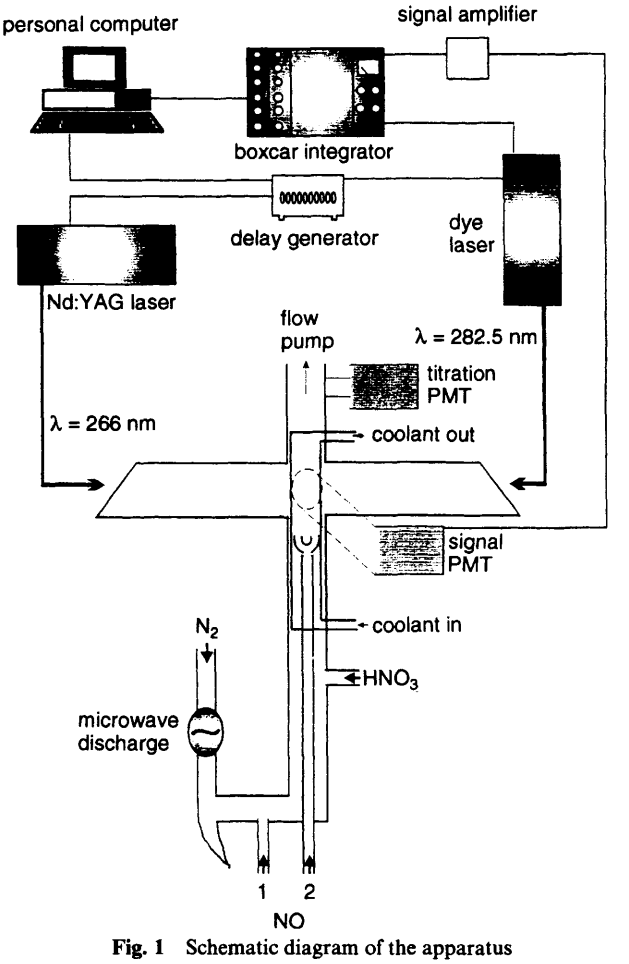

Fig. 1 Schematic diagram of the apparatus

The flow rate of the gas mixture could be adjusted by manipulating a large stopcock at the downstream end of the flow tube. A balance had to be struck between the requirements: (i) to minimise atom loss (see below) and condensation of the HNO_3 on the cold surfaces of the inserts and (ii) to maximise the time for the gas to equilibrate at the temperature of the cryogen. In addition, in the present experiments where the beams from the photolysis and probe lasers are perpendicular to the gas flow, the linear flow could not be too fast, or transport of OH radicals past the region illuminated by the probe laser would contribute a major, non-exponential, loss term to the background decay of the LIF signals. This compromise led us to use linear flow speeds of *ca.* 2 m s^{-1}. The temperatures which were achieved for particular combinations of cryogen and gas flow at the centre of the cross, where kinetic observations were actually made, could be measured by inserting a thermocouple probe either down the length of the main tube, using the moveable injector, or across the main tube, through one of the side-arms. These measurements indicated that the temperatures were constant to 1 K for ± 1 cm about the central axis of the tube and for at least ± 2 cm upstream and downstream of the point at which the laser beams crossed the gas flow. Using liquid nitrogen as the coolant, it was possible to reach 103 K, the lowest temperature in the present series of experiments. It is estimated that the temperatures which are cited below should be accurate to ± 4 K.

All gas flows were controlled by mass flow controllers. Nitrogen atoms were generated by passing N_2 through a microwave discharge applied in the side-arm leading to the main flow tube. A range of N atom concentrations was produced by altering the power applied to the discharge in the

range 25–120 W. The flow, and hence the concentration, of atomic nitrogen was determined by titration with NO.[44] NO could be added either at a fixed port (shown as point 1 in Fig. 1) on the side-arm upstream of the main reaction cell but downstream of the discharge cavity, or through the injector (point 2 in Fig. 1) which can be moved along the central axis of the main flow tube. The extent of the rapid titration reaction:

$$N + NO \rightarrow N_2 + O(^3P) \quad (3)$$

was followed by observing the chemiluminescent emissions from N_2, up to the titration end-point, and from NO_2, beyond the end-point, using a photomultiplier tube (EMI 9659QAM), placed on the main flow tube downstream from the observation point at the centre of the cross formed by the main flow tube and its side-arms. At the end-point, the emissions were extinguished. Reaction (3) was used not only to determine the steady-state concentration of N atoms, but also to convert those N atoms quantitatively to atomic oxygen.

Once a known steady-state concentration of N or O atoms had been established in the flowing gas, a small flow of HNO_3 diluted in argon was added just upstream of the first cooled section of the main flow tube. Since these genuine flow tube experiments used quite large gas flows, rather than pre-preparing an HNO_3–Ar mixture, a steady flow of argon was bubbled through a 1 : 2 mixture of concentrated nitric and sulfuric acids maintained at room temperature. The argon flow was kept as low as possible consistent with obtaining acceptable LIF signals from the OH radicals produced by PLP of the HNO_3.

A cruciform shape was adopted for the reaction cell for two reasons. First, it means that the time for which the radical precursor and the radical atoms are mixed can be minimised. Although this was unimportant in the present series of experiments, since any reaction between HNO_3 and N or O atoms seems to be very slow, it may become a real difficulty in other radical–radical systems which we plan to study. The second reason is pertinent to the present experiments. The present design of the reaction cell incorporates a moveable injector so that atom concentrations can be measured at various points along the flow tube. In the usual configuration for our low-temperature experiments,[43] the beams from the photolysis and probe lasers counterpropagate along the axis of the flow so that a moveable injector cannot be included in the apparatus. Measuring the concentrations of N and O atoms close to the reaction zone was important since they were found to decrease down the cooled section of the flow tube. The results of these experiments and visual inspection of afterglows in similar cross-shaped vessels suggests that there is negligible loss of atoms into the essentially static gas occupying the side-arms. These measurements, and the estimation of concentrations of atoms in the observation zone, are described separately in the next section of this paper.

The photolysis and probe laser beams entered the reaction cell in counterpropagating directions, and across the direction of the gas flow, *via* the two side-arms forming the cross. These side-arms were 30 mm id and *ca.* 30 cm long, and they carried baffles to reduce scattered laser light and fluorescence from the Spectrosil windows mounted, at Brewsters angle, at the end of each side-arm. Photolysis of HNO_3 to produce OH radicals was effected by the frequency-quadrupled output at 266 nm of a Nd : YAG laser (Spectron Lasers, model SL404) which operated at 10 Hz and gave *ca.* 15–20 mJ per pulse. The probe radiation was provided by a frequency-doubled dye laser (JK Lasers, system 2000) pumped by a frequency-doubled Nd : YAG laser (JK Lasers, DLPY4) which was tuned at *ca.* 282.5 nm to a rotational line in the (1, 0) band of the $A\,^2\Sigma^+$–$X\,^2\Pi$ system of OH. Fluorescence in the (1, 1) and (0, 0) bands was observed through two filters: a filter which eliminated radiation below *ca.* 295 nm (UHQ, WG295), and a narrow band interference filter with a bandpass of 10 nm centred at 310 nm (Ealing Electro-Optics, 35-8044).

The methods for controlling the delays between the pulses from the two lasers, for gathering and storing the LIF signals from OH and for fitting the decay traces were identical to those described in early papers from this laboratory.[43]

Results

Corrections for Atomic Recombination

Preliminary experiments, both in the present series and earlier,[45] showed that the concentrations of N and O atoms decreased as the gas mixture containing them flowed through the reaction cell. This effect increased as the temperature was lowered, was greater for O atoms than N atoms and could be affected by deposition of HNO_3 on the cold walls of the inserts carrying the cryogens. As has already been mentioned, to counter this last effect the flow of HNO_3 was kept to a minimum. Under our experimental conditions, there was no noticeable change in the rate constants for removal of OH which could be attributed to build-up of HNO_3 on the cold surfaces of the reactor.

To illustrate the need to guard against, or allow for, atom losses, the results of two series of experiments exploring such losses between titration point 1 and the reaction zone are shown in Fig. 2. Fig. 2(*a*) compares the N and O atom concentrations at these points at room temperature and 4 Torr total pressure, with a linear flow speed in the main flow tube of 1.1 m s^{-1}. The greater loss of O atoms is clearly evident. Fig. 2(*b*) compares the loss of O atoms in experiments at different temperatures using the same mass flow and total pressure in each case. The loss of atoms clearly increases as the temperature is lowered.

The rate constants for the gas-phase recombinations of N atoms[46] and of O atoms,[47] and their temperature dependence throughout most of the temperature range employed in our experiments, are well established, and hence the extent of atom loss by homogeneous, as distinct from heterogeneous, association could be estimated. Comparison with the measured losses (see below) suggests that gas-phase recombination was insignificant at room temperature, but that it could play a significant role at the lowest temperatures of our experiments.

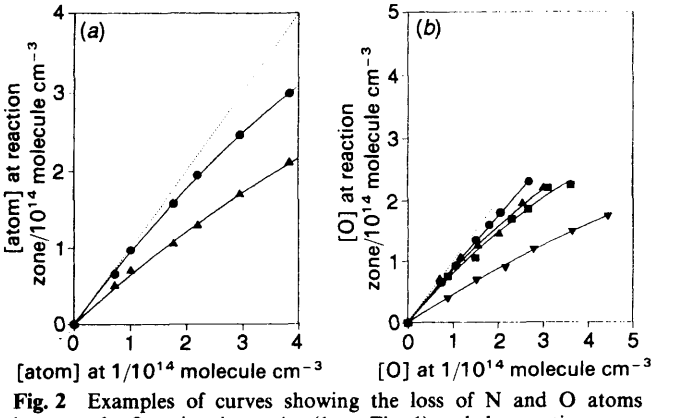

Fig. 2 Examples of curves showing the loss of N and O atoms between the first titration point (1 on Fig. 1) and the reaction zone. (*a*) Losses for (●) N atoms and (▲) O atoms at 294 K and a total pressure of 4 Torr, with a linear velocity in the main flow tube of 1.1 m s^{-1}. (*b*) Losses of O atoms at different temperatures: (●), 294 (▲), 227 (■) 190 and (▼) 158 K. The mass flow rate and the total pressure (2.5 Torr) was the same in each case.

It should be emphasised that the experimental conditions leading to the results shown in Fig. 2 were chosen to illustrate that atom losses occurred, not to minimise the effects of those losses. In the 'real' experiments, where OH decays were measured, conditions were chosen to reduce the effects of atom losses between the discharge and the LIF observation zone below those shown in Fig. 2. Thus, to minimise the time for homogeneous and heterogeneous reactions to occur, the linear flow rate was made as large as possible. Despite this precaution, atom losses were still significant. For N atoms, no correction for such loss was strictly necessary, as N + NO titrations could be performed by adding NO, *via* the moveable injector, directly into the zone where the side-arms cross the main flow tube, as well as at the fixed point 1, a few centimetres downstream from the discharge cavity. In both cases, the chemiluminescent emissions were observed using the photomultiplier tube near the downstream end of the main flow tube. In this way, a comparison could be made, for wide ranges of total pressure and temperature, between the concentrations of N atoms estimated by titration at point 1 and those actually present at the point where time-resolved experiments were carried out. Experiments like these were conducted with the moveable injector in the same position as in the LIF measurements on OH radical decays which are described in the next section of this paper. They enabled the required N atom concentrations to be determined from titrations carried out at the fixed titration point 1. The results for N + OH quoted in Table 1 include the results of experiments in which the concentrations of N atoms were estimated by both methods: 'direct' titration in the reaction zone, and titration at point 1 with subsequent correction for atom loss. In only four out of the 36 sets of experiments was the maximum correction for loss of N atoms greater than 16%. In the case of experiments at 103 K, where the losses of N atoms were quite extensive, their concentrations were assessed only by titration with NO added through the injector directly into the reaction zone.

The situation in respect of O atoms was rather different, and less favourable, partly because the losses were greater and partly because it was less straightfoward to estimate their concentration in the reaction zone. The latter difficulty arose because, in order to ensure complete mixing and hence quantitative conversion of N to O atoms by the reaction zone, it was necessary to add NO to the gas flow several centimetres upstream.

Therefore, in order to estimate the loss of O atoms between titration point 1 and the reaction zone, a method was adopted which was based on observing the NO_2 afterglow emission at the photomultiplier downstream from the reaction zone in two series of experiments. In each of the first set of measurements, the N atoms in the flowing gas were titrated against NO which was admitted to the reaction zone through the moveable injector. Then a known, small, excess of NO was added and the intensity of the NO_2 chemiluminescence was measured. By repeating this process for a number of atom concentrations and with the same excess [NO], a plot was obtained of the concentration of O atoms in the reaction zone against the intensity of the NO_2 emission.

Experiments in the second series were similar but now NO was added at the fixed titration point 1, just downstream of the discharge cavity. The titration end-point gave [O] at point 1, whilst the intensity of the NO_2 afterglow with the same excess [NO] present as before, by reference to the earlier graph of intensity against concentration, gave the concentration of O atoms in the reaction zone. The two sets of experiments enabled us to construct graphs of [O] at point 1 *vs.* [O] in the reaction zone for the ranges of total pressure and temperature used in the kinetics experiments. Only in one case (at 158 K) did the maximum correction for O atom loss exceed 35%. At 103 K, the loss of atomic oxygen was too great to make an acceptably accurate correction.

Kinetic Measurements on the Reactions of OH with N and O Atoms

A typical example of the LIF signal decays obtained in the present experiments is shown in Fig. 3. These observed signals were fitted to an exponential decay using a non-linear least-squares fitting program. Inspection of the residuals and autocorrelations, also provided by the computer program, confirmed that the experimental signals were accurately matched by a single-exponential decay function.

The pseudo-first-order rate constants (k_{1st}) obtained at a given temperature by fitting the experimental LIF signals in the manner just described were plotted against the concentrations of the radical atom making due allowance for atom loss. Examples of plots of k_{1st} *vs.* [N] and k_{1st} *vs.* [O] are given in Fig. 4. The gradients of these plots yield second-order rate constants for reactions (1) and (2). The number of runs and the conditions used for each combination of tem-

Table 1 Summary of experimental conditions and rate constants for N + OH and O + OH reactions[a]

T/K	no. of expts.	[N] or [O] /10^{14} molecule cm^{-3}	p/Torr	k_1 or k_2 /10^{-11} cm^3 molecule^{-1} s^{-1}
N + OH				
294	14	0.5–3.5	2.5–6.0	5.2 ± 0.3[b]
227	5	0.5–2.4	2.0–2.5	6.0 ± 0.4
190	9	0.6–2.2	1.5–2.5	6.4 ± 0.5
158	5	0.6–2.6	1.5–2.5	7.0 ± 0.6
103	3	0.25–1.5	1.0	8.0 ± 0.8
50	—	—	—	(10.2)[a]
10	—	—	—	(14.0)
O + OH				
294	11	0.5–2.9	2.5–4.0	4.2 ± 0.2
227	5	0.5–2.1	2.0–2.5	4.5 ± 0.3
190	9	0.5–2.0	1.5–2.5	5.2 ± 0.3
158	3	0.5–2.5	1.5–2.0	6.1 ± 0.6
103	—	—	—	(8.0)[a]
50	—	—	—	(11.1)
10	—	—	—	(16.0)

[a] Values given in brackets are estimated, using the method described in the text. [b] Weighted average of the individual determinations with errors quoted as single standard deviations.

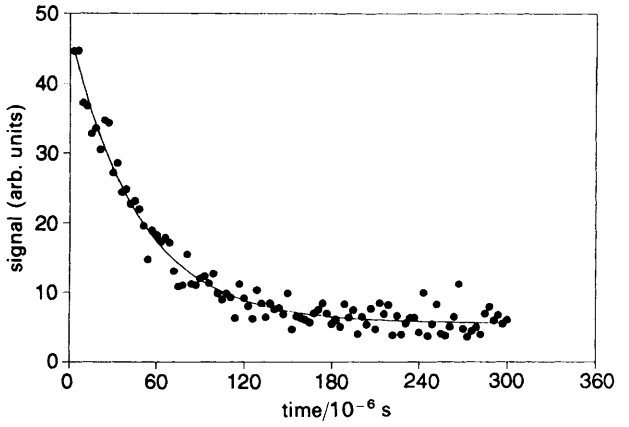

Fig. 3 Example of the decay of LIF signals from OH as the delay time between the pulses from the photolysis and probe lasers was increased. Temperature 103 K, total pressure 1.0 Torr and the concentration of N atoms 1.2×10^{14} molecule cm^{-3}.

perature and radical atom are summarised in Table 1, which also lists the average values of k_1 and k_2 at each temperature. The average values of the rate constants at each temperature were obtained by taking a weighted average of the individual values of $k_1(T)$ and $k_2(T)$ determined from plots of k_{1st} *vs.*

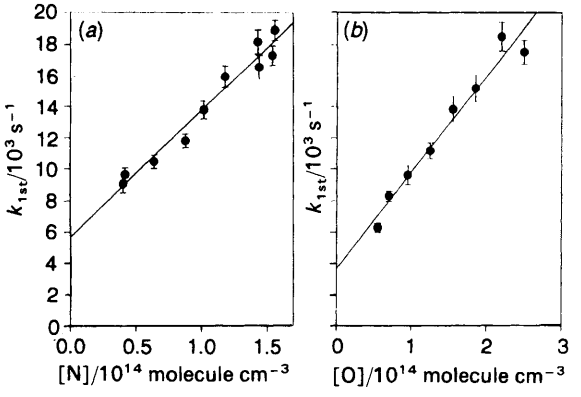

Fig. 4 Examples of the plots from which values of the second-order rate constants k_1 and k_2 were determined. Each panel shows the variation of the pseudo-first-order rate constants for decay in the LIF signal from OH: (*a*) with the concentration of N atoms, $T = 103$ K and $p = 1.0$ Torr; (*b*) with the concentration of O atoms, $T = 158$ K and $p = 1.5$ Torr.

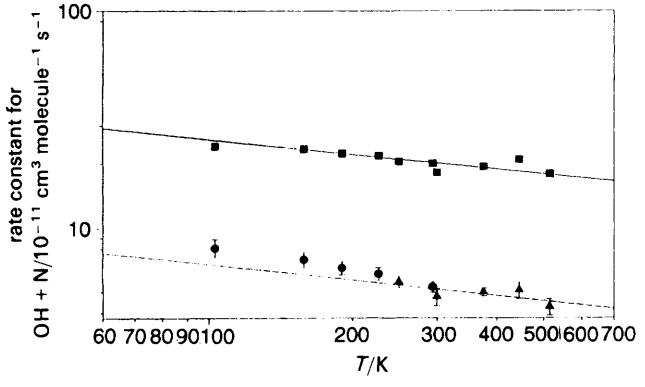

Fig. 5 log–log plot showing the variation of the rate constants for reaction between OH and N atoms with temperature. (●) Experimental rate constants observed in the present work and (▲) by Howard and Smith,[1] the line is their recommended fit. (■) Correspond to values of the hypothetical rate constants for reaction on the lowest potential-energy surface correlating with reagents and products (see text).

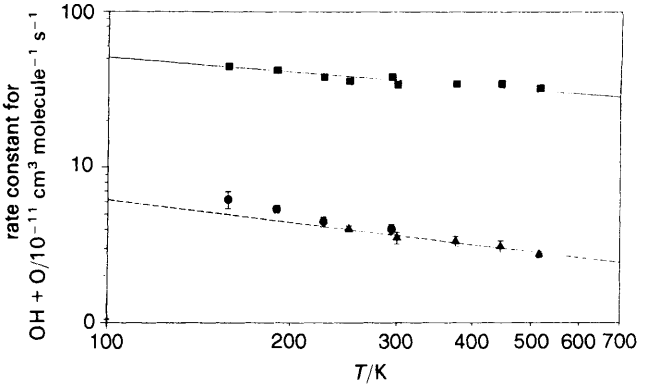

Fig. 6 log–log plot showing the variation of the rate constants for reaction between OH and O atoms with temperature. (●) Experimental rate constants observed in the present work and (▲) by Howard and Smith,[1] the line is their recommended fit. (■) Correspond to values of the hypothetical rate constants for reaction on the lowest potential-energy surface correlating with reagents and products (see text).

[N] or [O], like those shown in Fig. 4, the weighting factors being inversely proportional to the variances of the individual values. The errors quoted in Table 1 correspond to single standard deviations calculated from the weighted variance of the individual results.[48] The unweighted averages of the individual results and the standard deviations of these results about that mean value are very similar to the results summarised in Table 1. Errors in the corrections for atom loss were judged to be small relative to other errors. Moreover, they would show up in differences between the various values of the second-order rate constants determined at a particular temperature but under different flow conditions.

Finally, Fig. 5 and 6 display the temperature dependence of the observed rate constants. Where the present results overlap those obtained by Howard and Smith,[1] the agreement is excellent. The dashed lines represent the functions derived by Howard and Smith to match their experimental rate constants and given in the Introduction of the present paper. It is evident that k_1 and k_2 continue to increase as the temperature is lowered through the range covered in the present experiments and that the rates of these increases appear to be greater than predicted by the expressions given by Howard and Smith.

Discussion

The variation with temperature of the rate constants for reactions (1) and (2) can be considered to result from two effects. One factor arises from the temperature dependence of the reagent populations in different spin–orbit states, which changes the fraction of collisions which occur on the potential surface across which reaction takes place. In addition, there will be some temperature dependence resulting from the dynamics of the collisions on the reactive potential.

Quantum-chemical calculations suggest that, for both (1) and (2), reaction takes place over the lowest potential-energy surface which correlates adiabatically with reagents and products. In the case of reaction (1),[24] the symmetry of the surface is $^3A''$; for reaction (2),[27] the lowest energy surface has $^2A''$ symmetry. In the absence of non-adiabatic effects, an assumption which appears to be supported by the detailed study of the O(^{3}P) + OH reaction by Graff and Wagner,[49] the effect of electronic degeneracy and near-degeneracy in the reagents can be calculated by elementary statistical mechanics and allowed for by a factor (F_{el}), which is simply the ratio of the electronic degeneracy of the surface over which

reaction occurs to the product of the electronic partition functions of the reagents; *i.e.* $F_{el} = g_{el}^{\neq}/\Pi g_{el,i}$. Consequently, the effect of changes in this factor as the temperature is changed can be allowed for by dividing the observed rate constants by the appropriate value of F_{el}.†

This procedure yields rate constants (k'_1 and k'_2) relating only to those collisions whose dynamics are controlled by the lowest potential-energy surface. We have calculated values of these rate constants and examined their temperature dependence as shown in Fig. 5 and 6. Within experimental error these log–log plots are linear so that one can derive the following expressions for k_1 and k_2:

$$k_1(T) = F_{el}(T)(T/298)^{-0.17}2.0 \times 10^{-10} \text{ cm}^3 \text{ molecule}^{-1} \text{ s}^{-1}$$

$$k_2(T) = F_{el}(T)(T/298)^{-0.24}3.7 \times 10^{-10} \text{ cm}^3 \text{ molecule}^{-1} \text{ s}^{-1}$$

Our present results confirm that the rate constants for the reactions between the OH radical and the atomic radicals N(^{4}S) and O(^{3}P) continue to increase as the temperature is lowered, to 103 K in the case of reaction (1) between N atoms and OH, and to 158 K for O + OH, and that this temperature dependence is not due entirely to variations in the electronic factors F_{el}. The 'negative temperature dependences' which are observed for $k'_1(T)$ and $k'_2(T)$ are consistent with rate constants or cross-sections for reaction which are determined by the ability of the intermolecular potential at long and medium range to 'capture' the reagents and bring them into close collisions. It seems likely that, in keeping with other radical–radical systems,[50,51] the crucial part of the intermolecular potential only becomes that arising from the dispersion forces and the non-symmetric charge distributions on the reagents, at very low temperatures indeed. At higher temperatures, the crucial transition-state region moves to shorter inter-reagent separations, where chemical forces start to act and this change contributes to the decrease in the rate constants as the temperature is increased.

A major motivation for the present work has been the wish to provide a basis on which reasonably accurate estimates could be made of the rate constants for reactions (1) and (2) under the conditions prevailing in interstellar clouds. We believe that the analysis given above, in which the temperature effects due to changes in the fine structure populations are separated from those resulting from the dynamics on the potential-energy surface for reaction, provides such a basis. At $T \leqslant 50$ K, both O(^{3}P) atoms and OH(X $^2\Pi$) radicals will be predominantly (>99% and >98%, respectively) in their lowest spin–orbit state, if the populations are thermally equilibrated, so that the factors F_{el} become temperature independent and equal to 0.375 for reaction (1) and 0.2 for reaction (2) under interstellar conditions ($10 \leqslant T/\text{K} \leqslant 50$). Therefore, for the purposes of modelling interstellar cloud chemistry, the rate constant can be expressed in the form: $k(T) = AT^B$, with $A = 2.0 \times 10^{-10}$ cm^3 molecule^{-1} s^{-1}, $B = -0.17$ for the reaction between N atoms and OH, and $A = 3.7 \times 10^{-10}$ cm^3 molecule^{-1} s^{-1}, $B = -0.24$ for the O + OH reaction.

The effect that revised rate constants for neutral–neutral reactions can have on models of interstellar cloud chemistry can be dramatic. Until the mid-1980s, modellers used expressions for $k_1(T)$ and $k_2(T)$ with a positive ($T^{1/2}$) temperature dependence,[7,8] which yielded rate constants at 10 K roughly 1/20th of the estimated values which are given in Table 1. Since then, values of $k_1(T)$ and $k_2(T)$ based on the rate expressions given by Howard and Smith[1] have been incorporated into a number of models.[9–13] Here, we cite three examples of the results of such revised calculations.

First, based on Howard and Smith's rate constant for reaction (1), Tarafdar and Dalgarno[11] argue that the reaction between N atoms and OH is the principal source of NO in diffuse interstellar clouds, although they note that the concentrations of NO estimated on this basis are in poor agreement with those inferred from observations on the ζ Ophiuchi cloud. Secondly, Nercessian *et al.*[12] have estimated that the number density of OH in a molecular cloud near the star HD-29647 drops by an order of magnitude when rate constants are used for reaction (1) based on the expression of Howard and Smith.[1] This change improves the agreement with observation. Finally, we point to a paper by Davidsson and Stenholm.[36] In addition to using classical trajectory methods, an extended Langevin model and Howard and Smith's experimental results in order to estimate values of $k_2(T)$ in the temperature range appropriate to interstellar clouds, they discussed the implications for interstellar chemistry of larger low-temperature rates for the O + OH reaction, particularly problems associated with the non-detection of O_2 in interstellar clouds.

Although the present experimental results and the proposed method of extrapolation provide a reasonable basis for the estimated rate constants which are given in Table 1, there is, of course, no substitute for direct laboratory measurements at the ultra-low temperatures of interstellar clouds. At present, the best hope for such measurements would seem to lie with the CRESU method.[40] However, application of this technique to reactions involving two unstable radical species is likely to prove very difficult, as it will be necessary to generate one of the radicals in a large known concentration. Until such time as results from direct measurements at ultra-low temperatures become available, we suggest that the rate constants estimated in this paper should be employed in astrochemical models.

Summary

Using a combination of pulsed laser photolysis and discharge-flow techniques in a cryogenically cooled reaction vessel, it has proved possible to obtain rate constants for the reactions of OH radicals with N atoms down to 103 K and with O atoms down to 158 K. These experiments significantly increase the temperature range for which direct kinetic data for these reactions have been measured. The rate constants for both reactions increase monotonically as the temperature is lowered. By factorising out effects due to the temperature dependence of the reagent populations in different fine structure states, the rate constants for both reactions obtained in the present work and in the experiments of Howard and Smith[1] can be fitted to a relatively simple expression. It is suggested that this fit can be used to make accurate estimates of the rate constants for reactions (1) and (2) at ultra-low temperatures and hence provide values of $k_1(T)$ and $k_2(T)$ which can be used in chemical models of molecular synthesis in interstellar clouds.

We thank SERC and CEC, under its Science Plan programme, for support of our work on gas-phase kinetics at low temperature. D.W.A.S. is also grateful to SERC for the award of a research studentship. We acknowledge the assistance of Ken Boyle with some of the experimental measurements reported in this paper. We thank Professor George Schatz for preprints of his papers, ref. 20 and 27.

† For OH, g_{el} is calculated by summing the populations in the rotational levels of the two spin–orbit states and evaluating g_{el} as $2(1 + f')$ where f' is the ratio of the populations in the upper and lower sets of levels.

References

1 (*a*) M. J. Howard and I. W. M. Smith, *Chem. Phys. Lett.*, 1980, **69**, 40; (*b*) M. J. Howard and I. W. M. Smith, *J. Chem. Soc., Faraday 2*, 1981, **77**, 997.
2 R. S. Lewis and R. T. Watson, *J. Phys. Chem.*, 1980, **84**, 3495.
3 W. H. Brune, J. J. Schwab and J. G. Anderson, *J. Phys. Chem.*, 1983, **87**, 4503.
4 (*a*) R. Atkinson, D. L. Baulch, R. A. Cox, R. F. Hampson Jr., J. A. Kerr and J. Troe, *J. Phys. Chem. Ref. Data*, 1989, **18**, 881; (*b*) R. Atkinson, D. L. Baulch, R. A. Cox, R. F. Hampson Jr., J. A. Kerr and J. Troe, *J. Phys. Chem. Ref. Data*, 1992, **21**, 1125.
5 J. A. Miller, R. J. Kee and C. Westbrook, *Annu. Rev. Phys. Chem.*, 1990, **41**, 345.
6 R. P. Wayne, *Chemistry of Atmospheres*, Clarendon Press, Oxford, 2nd edn., 1991.
7 S. Prasad and W. T. Huntress Jr., *Astrophys. J. Suppl. Ser.*, 1980, **43**, 1.
8 T. E. Graedel, W. D. Langer and M. A. Frerking, *Astrophys. J. Suppl. Ser.*, 1982, **48**, 321.
9 Y. P. Viala, *Astron. Astrophys. Suppl. Ser.*, 1986, **64**, 391.
10 G. Pineau des Forêts, E. Roueff and D. R. Flower, *Mon. Not. Roy. Astron. Soc.*, 1990, **244**, 668.
11 S. P. Tarafdar and A. Dalgarno, *Astron. Astrophys.*, 1990, **232**, 239.
12 E. Nercessian, J. J. Benayoun and V. P. Viala, *Astron. Astrophys.*, 1988, **195**, 245.
13 R. D. Brown and E. H. N. Rice, *Mon. Not. Roy. Astron. Soc.*, 1986, **223**, 405.
14 I. W. M. Smith, *J. Chem. Soc., Faraday Trans.*, 1991, **87**, 2271.
15 G. A. Gallup, *Inorg. Chem.*, 1975, **14**, 563.
16 (*a*) P. J. Bruna and C. M. Marian, *Chem. Phys. Lett.*, 1979, **67**, 109; (*b*) P. J. Bruna, *Chem. Phys.*, 1980, **49**, 39.
17 (*a*) S. P. Walch and C. M. Rohlfing, *J. Chem. Phys.*, 1989, **91**, 2939.
18 T. J. Lee, *J. Chem. Phys.*, 1993, **99**, 9783.
19 F. Pauzat, Y. Ellinger, G. Berthier, M. Gérin and Y. Viala, *Chem. Phys.*, 1993, **174**, 71.
20 R. Guadagnin, G. C. Schatz and S. P. Walch, *J. Chem. Phys.*, 1994, in the press.
21 C. F. Melius and R. J. Blint, *Chem. Phys. Lett.*, 1979, **64**, 183.
22 S. R. Langhoff and R. L. Jaffe, *J. Chem. Phys.*, 1979, **71**, 1475.
23 T. H. Dunning, Jr., S. P. Walch and M. M. Goodgame, *J. Chem. Phys.*, 1981, **74**, 3482.
24 S. P. Walch, C. M. Rohlfing, C. F. Melius and C. W. Bauschlicher Jr., *J. Chem. Phys.*, 1988, **88**, 6273.
25 A. J. C. Varandas, J. Brandão and L. A. M. Quintales, *J. Phys. Chem.*, 1988, **92**, 3732.
26 D. C. Clary, *Annu. Rev. Phys. Chem.*, 1990, **41**, 61.
27 R. Guadagnin and G. C. Schatz, *J. Chem. Phys.*, 1994, in the press.
28 (*a*) J. A. Miller, *J. Chem. Phys.*, 1981, **74**, 5120; 1981, **75**, 5349; (*b*) J. A. Miller, *J. Chem. Phys.*, 1986, **84**, 6170.
29 (*a*) L. A. M. Quintales, A. J. C. Varandas and J. M. Alvarino, *J. Phys. Chem.*, 1988, **92**, 4552; (*b*) A. J. C. Varandas, J. Brandao and M. R. Pastrana, *J. Chem. Phys.*, 1992, **96**, 5137; (*c*) A. J. C. Varandas, *J. Chem. Phys.*, 1992, **97**, 4050.
30 (*a*) N. Markovic, G. Nyman and S. Nordholm, *Chem. Phys. Lett.*, 1989, **159**, 435; (*b*) G. Nyman and J. Davidsson, *J. Chem. Phys.*, 1990, **92**, 2415.
31 D. C. Clary and H-J. Werner, *Chem. Phys. Lett.*, 1984, **112**, 346.
32 S. N. Rai and D. G. Truhlar, *J. Chem. Phys.*, 1983, **79**, 6046.
33 J. Troe, *J. Phys. Chem.*, 1986, **90**, 3485.
34 D. C. Clary, *Mol. Phys.*, 1984, **53**, 3.
35 (*a*) L. F. Phillips, *Chem. Phys. Lett.*, 1990, **165**, 545; (*b*) L. F. Phillips, *J. Phys. Chem.*, 1990, **94**, 7482.
36 J. Davidsson and L. G. Stenholm, *Astron. Astrophys.*, 1990, **230**, 504.
37 I. W. M. Smith, R. P. Tuckett and C. J. Whitham, *J. Chem. Phys.*, 1993, **98**, 6267.
38 M. Quack and J. Troe, *Ber Bunsenges, Phys. Chem.*, 1976, **80**, 1140.
39 (*a*) P. Pechukas, J. C. Light and C. Rankin, *J. Chem. Phys.*, 1966, **44**, 794; (*b*) J. C. Light, *Discuss. Faraday Soc.*, 1967, **44**, 14.
40 (*a*) I. R. Sims, J-L. Queffelec, A. Defrance, C. Rebrion-Rowe, D. Travers, B. R. Rowe and I. W. M. Smith, *J. Chem. Phys.*, 1992, **97**, 8798; (*b*) I. R. Sims, J-L. Queffelec, A. Defrance, C. Rebrion-Rowe, D. Travers, P. Bocherel, B. R. Rowe and I. W. M. Smith, *J. Chem. Phys.*, 1994, **100**, 4229; (*c*) I. R. Sims, J-L. Queffelec, A. Defrance, D. Travers, B. R. Rowe, L. Herbert, J. Karthauser and I. W. M. Smith, *Chem. Phys. Lett.*, 1993, **211**, 461.
41 (*a*) I. R. Sims, P. Bocherel, A. Defrance, D. Travers, B. R. Rowe and I. W. M. Smith, *J. Chem. Soc., Faraday Trans.*, 1994, **90**, 1473; (*b*) I. R. Sims, I. W. M. Smith, D. C. Clary, P. Bocherel and B. R. Rowe, *J. Chem. Phys.*, 1994, **101**, 1748.
42 B. R. Rowe, I. R. Sims, P. Bocherel and I. W. M. Smith, *Am. Inst. Phys. Conf. Proc.*, 1994, in the press.
43 (*a*) M. J. Frost, P. Sharkey and I. W. M. Smith, *Faraday Discuss. Chem. Soc.*, 1991, **91**, 305; (*b*) P. Sharkey and I. W. M. Smith, *J. Chem. Soc., Faraday Trans.*, 1993, **89**, 631; (*c*) M. J. Frost, P. Sharkey and I. W. M. Smith, *J. Phys. Chem.*, 1993, **97**, 12254; (*d*) C. M. Moore, I. W. M. Smith and D. W. A. Stewart, *Int. J. Chem. Kinet.*, 1994, **26**, 813.
44 M. A. A. Clyne in *Reactive Intermediates in the Gas Phase*, ed. D. W. Setser, Academic Press, 1979, ch. 1.
45 M. J. Frost, P. Sharkey and I. W. M. Smith, unpublished results.
46 W. Brennen and E. C. Shane, *J. Phys. Chem.*, 1971, **75**, 1552.
47 I. M. Campbell and C. N. Gray, *Chem. Phys. Lett.*, 1973, **18**, 607.
48 M. J. Pilling in *Modern Gas Kinetics: Theory, Experiment and Applications*, ed. M. J. Pilling and I. W. M. Smith, Blackwells, Oxford, 1987.
49 M. M. Graff and A. F. Wagner, *J. Chem. Phys.*, 1990, **92**, 2423.
50 S. J. Klippenstein and Y-W. Kim, *J. Chem. Phys.*, 1993, **99**, 5790.
51 I. W. M. Smith in *The Chemical Kinetics and Dynamics of Small Radicals*, ed. K. Liu and A. Wagner, World Scientific, Singapore, 1994, in the press.

Paper 4/04127E; *Received* 6*th July*, 1994